

**Supplementary Information**

**NiMn Layered Double Hydroxide as Efficient Electrocatalyst for Oxygen**

**Evolution Reaction and its Application in Rechargeable Zn-Air Batteries**

Afriyanti Sumboja,<sup>[a]</sup> Jingwei Chen,<sup>[b]</sup> Yun Zong,\*<sup>[a]</sup> Pooi See Lee,\*<sup>[b]</sup> and Zhaolin Liu\*<sup>[a]</sup>

<sup>a</sup> Institute of Materials Research and Engineering (IMRE), A\*STAR (Agency for Science, Technology and Research), 2 Fusionopolis Way, Innovis, #08-03, Singapore 138634

<sup>b</sup> School of Materials Science and Engineering, Nanyang Technological University, 50 Nanyang Avenue, Blk N4.1, Singapore 639798

\*Email: [zl-liu@imre.a-star.edu.sg](mailto:zl-liu@imre.a-star.edu.sg); [pslee@ntu.edu.sg](mailto:pslee@ntu.edu.sg); [y-zong@imre.a-star.edu.sg](mailto:y-zong@imre.a-star.edu.sg)

## 1. EDX mapping of $\text{Ni}_1\text{Mn}_1$ and $\text{Ni}_5\text{Mn}_1$

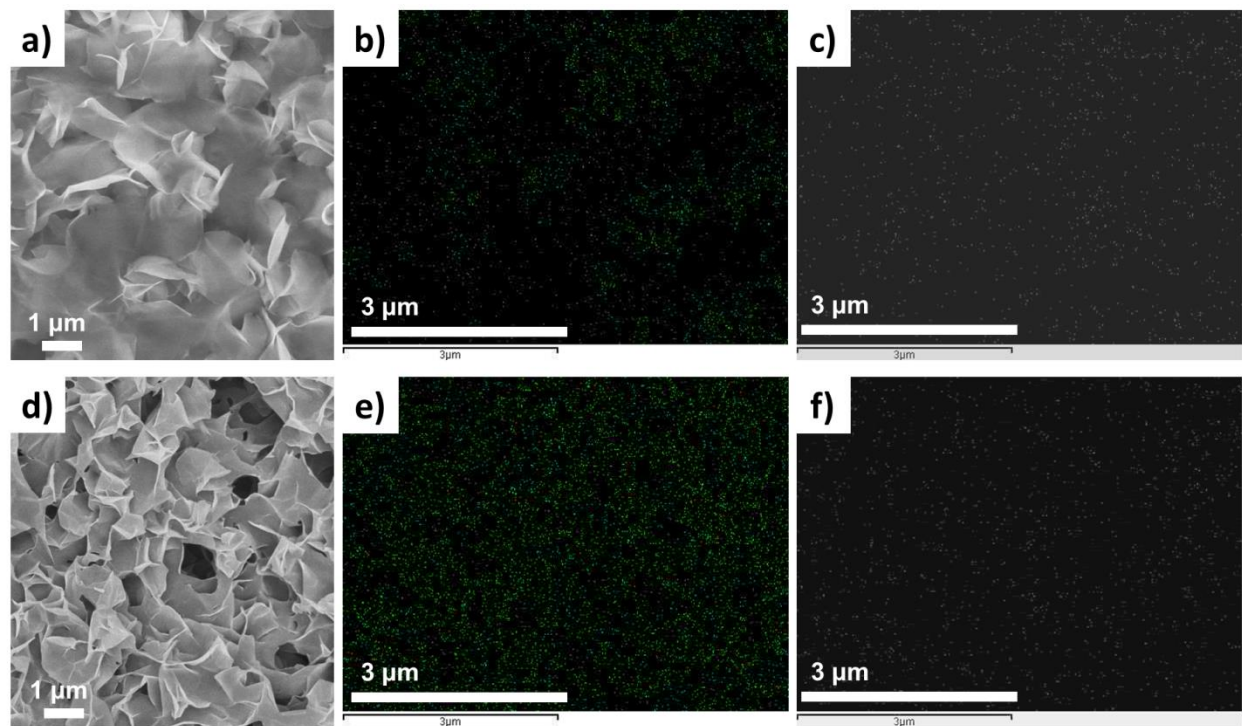


**Fig. S1** (a) SEM images of  $\text{Ni}_1\text{Mn}_1$  and EDX elemental mapping of (b) Ni and (c) Mn in  $\text{Ni}_1\text{Mn}_1$ . (d) SEM images of  $\text{Ni}_5\text{Mn}_1$  and EDX elemental mapping of (e) Ni and f) Mn in  $\text{Ni}_5\text{Mn}_1$ .

Ni and Mn in NiMn LDHs are atomically well-dispersed throughout the sample rather than forming separate phases, which further support our XRD results.

## 2. TEM of $\text{Ni}_1\text{Mn}_1$ and $\text{Ni}_5\text{Mn}_1$

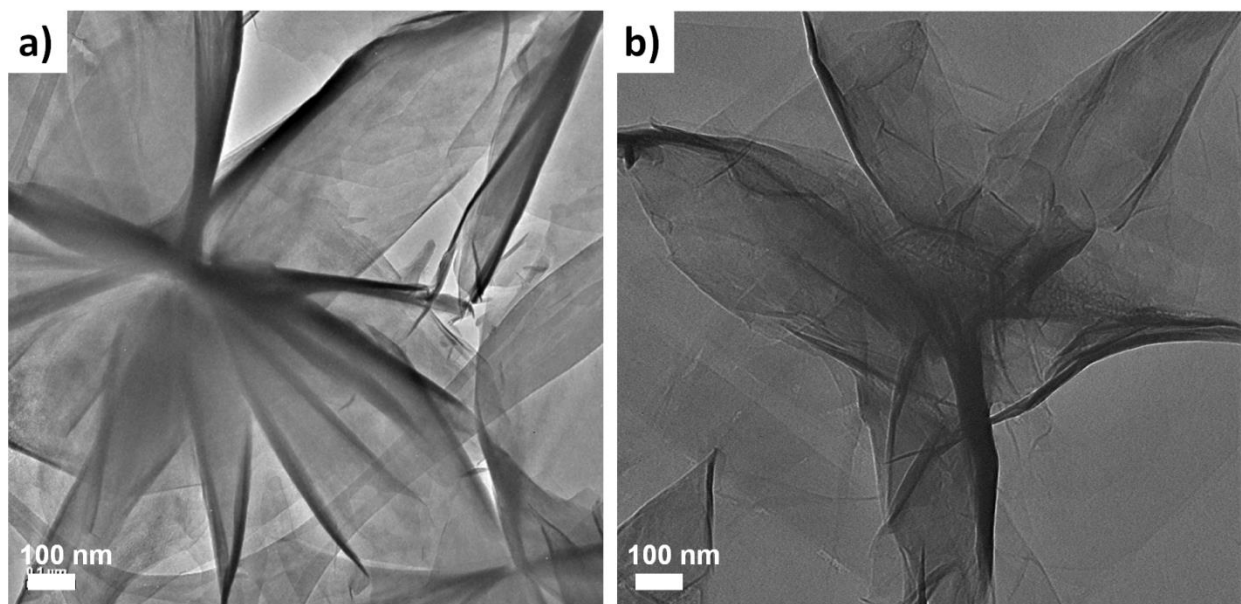


**Fig. S2** TEM images of (a)  $\text{Ni}_1\text{Mn}_1$  and (b)  $\text{Ni}_5\text{Mn}_1$

### 3. Characterization of commercial $\text{Ni(OH)}_2$

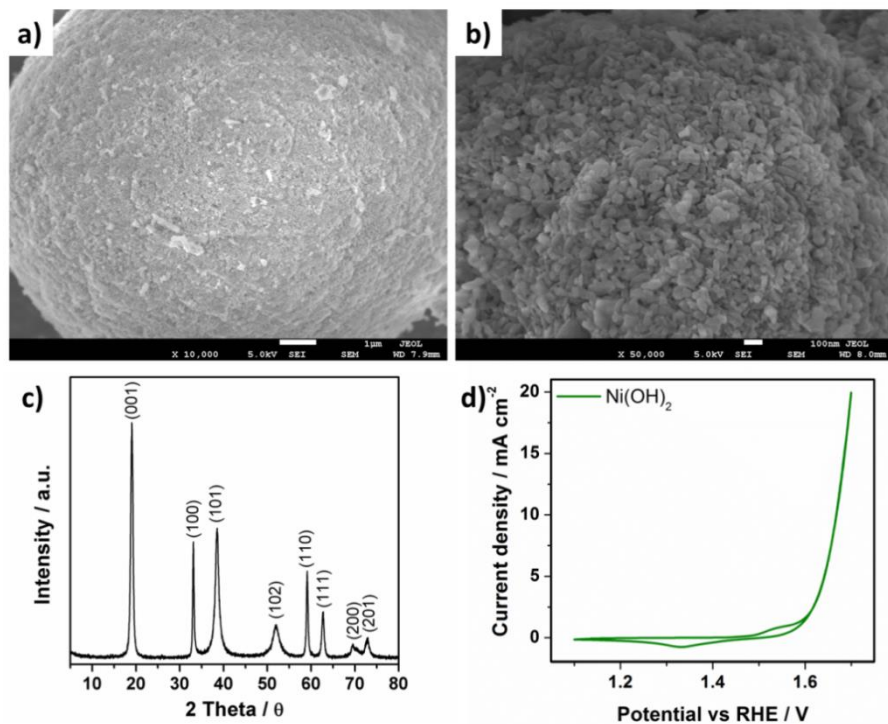


**Fig. S3** (a, b) SEM images and (c) XRD pattern commercial  $\text{Ni(OH)}_2$ . (d) RDE Cyclic voltammograms of commercial  $\text{Ni(OH)}_2$  at scan rate of  $5 \text{ mV s}^{-1}$  and rotating speed of 1600 rpm in 1 M KOH.

**4. Catalytic activity of 20 wt% Ni<sub>3</sub>Mn<sub>1</sub>/C, commercial 20 wt% RuO<sub>2</sub>/C and 20 wt% Ir/C during oxygen evolution reaction**

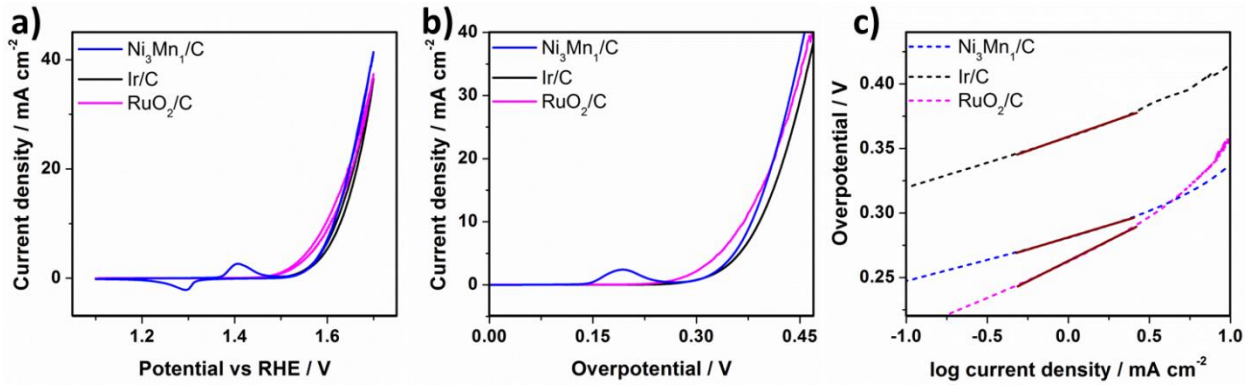


**Fig. S4** (a) Cyclic voltammograms and (b) linear scan voltammograms of 20 wt% Ni<sub>3</sub>Mn<sub>1</sub>/C, commercial 20 wt% Ir/C, and 20 wt% RuO<sub>2</sub> catalysts. (c) Tafel plots (i.e. dash curves) showing the Tafel slope (i.e. solid curve) of the samples.

In order to have fair comparison to 20 wt% Ir/C, we have also tested 20 wt% Ni<sub>3</sub>Mn<sub>1</sub>/C and 20 wt% RuO<sub>2</sub>/C. With 80 wt% of carbon black, the overpotential of RuO<sub>2</sub>, Ni<sub>3</sub>Mn<sub>1</sub>, and Ir are 0.37, 0.38, and 0.39 V, respectively. The Tafel plot of RuO<sub>2</sub>/C, Ni<sub>3</sub>Mn<sub>1</sub>/C and Ir/C are 63, 38, and 44 mV dec<sup>-1</sup>.

## 5. Stability of commercial RuO<sub>2</sub>

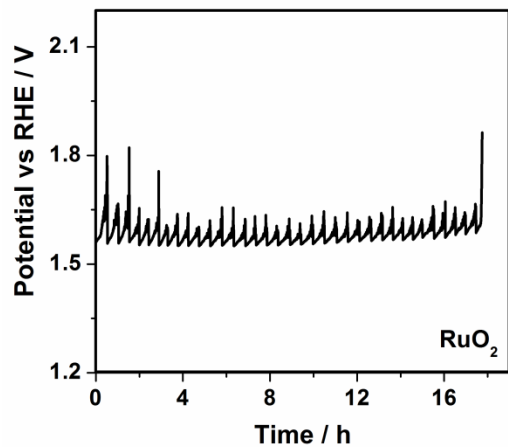


**Fig. S5** Stability test of commercial RuO<sub>2</sub> under constant current of 10 mA cm<sup>-2</sup> at rotating speed of 2500 rpm in 1 M KOH.

Due to the low overpotential of RuO<sub>2</sub> at 10 mA cm<sup>-2</sup>, O<sub>2</sub> gas generated at the surface of RDE glassy carbon is considerably high causing significant fluctuation in the measured potential.

## 6. Catalytic activity of $\text{Ni}_3\text{Mn}_1$ LDH during oxygen reduction reaction

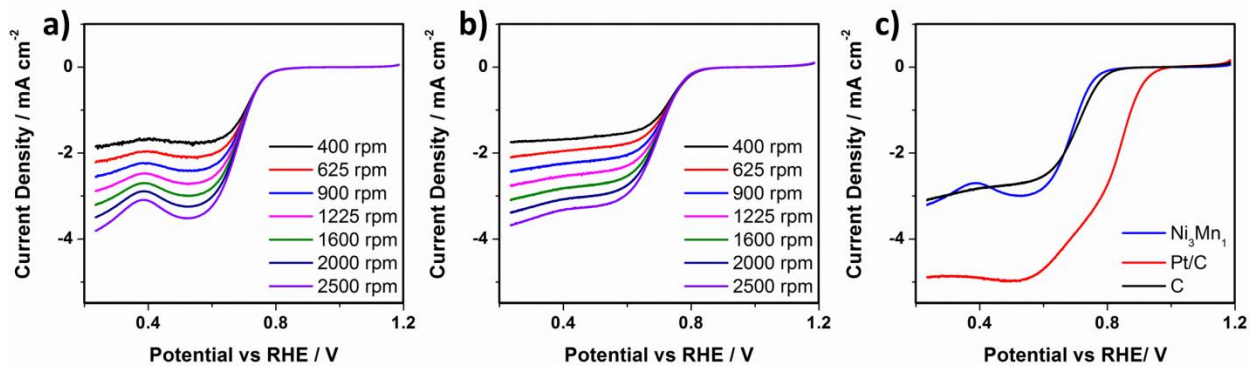


**Fig. S6** Linear scan voltammograms of (a)  $\text{Ni}_3\text{Mn}_1$  and (b) Vulcan carbon black during oxygen reduction reaction at various rotating speeds. (b) Linear scan voltammograms of  $\text{Ni}_3\text{Mn}_1$ , commercials Pt/C and Vulcan carbon black during oxygen reduction reaction at rotating speed of 1600 rpm. The measurements were carried out at scan rate of  $5 \text{ mV s}^{-1}$  in 0.1 M KOH.

A catalyst for oxygen reduction reaction (ORR) is required during the discharge of Zn-air batteries. Carbon black which is present in the carbon paper and catalyst ink of both batteries functions as ORR catalyst. Besides that, NiMn LDHs also show catalytic activity during oxygen reduction reaction in 0.1 M KOH (Fig. S4a). The catalytic activity of  $\text{Ni}_3\text{Mn}_1$  is inferior than 20 wt % Pt/C and similar to Vulcan carbon black.

## 7. Digital image of Zn-air batteries

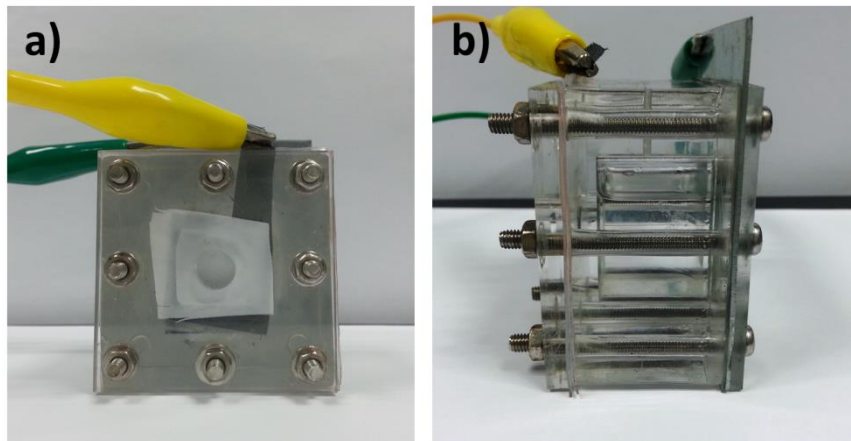


**Fig. S7** (a) Front view displaying the carbon paper air cathode. O<sub>2</sub> was supplied through the hole ( $\approx 0.79$  cm<sup>2</sup>); (b) Side view showing electrolyte and zinc plate anode. The cell contains 20 ml of electrolyte. Outer dimension of the cell is 6x6x4 cm<sup>3</sup>. The distance between air cathode and Zn-anode is about xx cm. The white color membrane is hydrophobic PTFE membrane which is used to prevent the leakage of the electrolyte during the prolonged cycling test.

## 8. Ni-based layered double hydroxide as OER catalyst in literature

**Table S1.** Ni-based layered double hydroxide as OER catalyst in literature

Ref	Catalyst	Overpotential at 10 mA cm <sup>-2</sup> (V)	Tafel Slope (mV dec <sup>-1</sup> )	Stability / Testing condition
This work	NiMn LDH	0.35	40	16 h / constant current at 10 mA cm <sup>-2</sup>
	Ir/C reference	0.39	44	
	RuO <sub>2</sub> reference	0.32	49	
<sup>1</sup>	NiFe LDH	0.35	47	-
<sup>2</sup>	Exfoliated NiFe LDH	0.302	40	13 h / constant current at 10 mA cm <sup>-2</sup>
	NiCo LDH	0.334	41	
	CoCo LDH	0.353	45	
	IrO <sub>2</sub> reference	0.338	47	
<sup>3</sup>	NiFe LDH on Ni foam	0.28	50	10 h / constant potential at 1.6 V (RHE)
<sup>4</sup>	CoMn LDH /MWCNT	0.30	73.6	12 h / constant current at 10 mA cm <sup>-2</sup>
	NiMn LDH /MWCNT	0.35	83.5	9 h / constant current at 10 mA cm <sup>-2</sup>
<sup>5</sup>	NiMn LDH	0.36	65	1 h / constant current at 5 mA cm <sup>-2</sup>
	NiMn LDH /rGO	0.26	46	2 h / constant current at 5 mA cm <sup>-2</sup>
<sup>6</sup>	NiCo LDH on carbon paper	0.37	40	6 h / constant current at 10 mA cm <sup>-2</sup>
<sup>7</sup>	NiCo LDH on Ni foam	0.42	113	1 h / constant potential at 1.52 V (RHE)
	RuO <sub>2</sub> reference	0.41	128	
<sup>8</sup>	NiCoFe LDH on Ni foam	0.23	53	10 h / constant potential at 1.46 V (RHE)
<sup>9</sup>	NiCo DH/N- graphene on Ni	0.35	614	12 h / constant potential at 1.54 V (RHE)

	foam				
<sup>10</sup>	NiFe DH/graphene on Ni foam	0.2	40	-	

## 9. Performance of rechargeable Zn-air batteries in literature

**Table S2.** Performance of rechargeable Zn-air batteries in literature

Ref	OER Catalyst	Initial charging voltage (V)	No. of Cycle	Applied Current (mA cm <sup>-2</sup> )	Change in charging voltage (%)
This work	NiMn LDH	1.98	200	10	5.4
<sup>11</sup>	MnO <sub>x</sub> /carbon paper	2.06	500	7.5	8
<sup>12</sup>	LaNiO <sub>3</sub> /N-CNT	2.17	10	17.6	~0
<sup>13</sup>	CoO/N-CNT/NiFe LDH	1.99	58	10	~0
<sup>14</sup>	MnO <sub>2</sub> /N-CNT	2.6	50	8	5
<sup>15</sup>	NiCo <sub>2</sub> O <sub>4</sub>	1.8	50	20	2.2
<sup>16</sup>	Co <sub>3</sub> O <sub>4</sub> /carbon nanofiber	2.03	55	20	-
<sup>17</sup>	Co <sub>3</sub> O <sub>4</sub> / MnO <sub>2</sub>	2.2	60	15	5
<sup>18</sup>	Co <sub>3</sub> O <sub>4</sub>	2.15	60	17.6	~0
<sup>19</sup>	αMnO <sub>2</sub> /LaNiO <sub>3</sub> /CNT	1.95	75	-	4.8
<sup>20</sup>	LaNiO <sub>3</sub> /N-CNT	2.15	75	17.6	4.5
<sup>21</sup>	Ag/MnO <sub>2</sub>	2.5	270	5 mA	~0
<sup>22</sup>	MnCo <sub>2</sub> O <sub>4</sub> /CNT	2.0	64	10	4.9
<sup>23</sup>	Mn-Co substituted Fe <sub>3</sub> O <sub>4</sub> / N-RGO	2.35	75	10	-

## References

1. K. Yan, T. Lafleur, J. Chai and C. Jarvis, *Electrochem. Commun.*, 2016, **62**, 24-28.
2. F. Song and X. Hu, *Nat. Commun.*, 2014, **5**.
3. Z. Lu, W. Xu, W. Zhu, Q. Yang, X. Lei, J. Liu, Y. Li, X. Sun and X. Duan, *Chem. Commun.*, 2014, **50**, 6479-6482.
4. G. Jia, Y. Hu, Q. Qian, Y. Yao, S. Zhang, Z. Li and Z. Zou, *ACS Appl. Mater. Interfaces*, 2016.
5. W. Ma, R. Ma, J. Wu, P. Sun, X. Liu, K. Zhou and T. Sasaki, *Nanoscale*, 2016, **8**, 10425-10432.
6. H. Liang, F. Meng, M. Cabán-Acevedo, L. Li, A. Forticaux, L. Xiu, Z. Wang and S. Jin, *Nano Lett.*, 2015, **15**, 1421-1427.
7. J. Jiang, A. Zhang, L. Li and L. Ai, *J. Power Sources*, 2015, **278**, 445-451.
8. Q. Yang, T. Li, Z. Lu, X. Sun and J. Liu, *Nanoscale*, 2014, **6**, 11789-11794.
9. S. Chen, J. Duan, M. Jaroniec and S. Z. Qiao, *Angew. Chem. Int. Ed.*, 2013, **52**, 13567-13570.
10. X. Long, J. Li, S. Xiao, K. Yan, Z. Wang, H. Chen and S. Yang, *Angew. Chem.*, 2014, **126**, 7714-7718.
11. A. Sumboja, X. Ge, F. W. T. Goh, B. Li, D. Geng, T. S. A. Hor, Y. Zong and Z. Liu, *ChemPlusChem*, 2015, **80**, 1341-1346.
12. D. U. Lee, H. W. Park, M. G. Park, V. Ismayilov and Z. Chen, *ACS Appl. Mater. Interfaces*, 2014, **7**, 902-910.
13. Y. Li, M. Gong, Y. Liang, J. Feng, J. E. Kim, H. Wang, G. Hong, B. Zhang and H. Dai, *Nat. Commun.*, 2013, **4**, 1805.
14. Z. Chen, A. Yu, R. Ahmed, H. Wang, H. Li and Z. Chen, *Electrochim. Acta*, 2012, **69**, 295-300.
15. M. Prabu, K. Ketpang and S. Shanmugam, *Nanoscale*, 2014, **6**, 3173-3181.
16. B. Li, X. Ge, F. W. T. Goh, T. S. A. Hor, D. Geng, G. Du, Z. Liu, J. Zhang, X. Liu and Y. Zong, *Nanoscale*, 2015, **7**, 1830-1838.
17. G. Du, X. Liu, Y. Zong, T. S. A. Hor, A. Yu and Z. Liu, *Nanoscale*, 2013, **5**, 4657-4661.
18. D. U. Lee, J. Scott, H. W. Park, S. Abureden, J.-Y. Choi and Z. Chen, *Electrochem. Commun.*, 2014, **43**, 109-112.
19. H. Ma and B. Wang, *RSC Adv.*, 2014, **4**, 46084-46092.
20. Z. Chen, A. Yu, D. Higgins, H. Li, H. Wang and Z. Chen, *Nano Lett.*, 2012, **12**, 1946-1952.
21. F. W. T. Goh, Z. Liu, X. Ge, Y. Zong, G. Du and T. S. A. Hor, *Electrochim. Acta*, 2013, **114**, 598-604.
22. X. Ge, Y. Liu, F. W. T. Goh, T. S. A. Hor, Y. Zong, P. Xiao, Z. Zhang, S. H. Lim, B. Li, X. Wang and Z. Liu, *ACS Appl. Mater. Interfaces*, 2014, **6**, 12684-12691.
23. Y. Zhan, C. Xu, M. Lu, Z. Liu and J. Y. Lee, *J. Mater. Chem. A*, 2014, **2**, 16217-16223.